

Long-term recording of external urethral sphincter EMG activity in unanesthetized, unrestrained rats

Brandon K. LaPallo,² Jonathan R. Wolpaw,^{1,2} Xiang Yang Chen,^{1,2} and Jonathan S. Carp^{1,2}

¹Wadsworth Center, New York State Department of Health, Albany, New York; and ²School of Public Health, SUNY at Albany, Rensselaer, New York

Submitted 23 January 2014; accepted in final form 26 June 2014

LaPallo BK, Wolpaw JR, Chen XY, Carp JS. Long-term recording of external urethral sphincter EMG activity in unanesthetized, unrestrained rats. *Am J Physiol Renal Physiol* 307: F485–F497, 2014. First published July 2, 2014; doi:10.1152/ajprenal.00059.2014.—The external urethral sphincter muscle (EUS) plays an important role in urinary function and often contributes to urinary dysfunction. EUS study would benefit from methodology for longitudinal recording of electromyographic activity (EMG) in unanesthetized animals, but this muscle is a poor substrate for chronic intramuscular electrodes, and thus the required methodology has not been available. We describe a method for long-term recording of EUS EMG by implantation of fine wires adjacent to the EUS that are secured to the pubic bone. Wires pass subcutaneously to a skull-mounted plug and connect to the recording apparatus by a flexible cable attached to a commutator. A force transducer-mounted cup under a metabolic cage collected urine, allowing recording of EUS EMG and voided urine weight without anesthesia or restraint. Implant durability permitted EUS EMG recording during repeated (up to 3 times weekly) 24-h sessions for more than 8 wk. EMG and voiding properties were stable over weeks 2–8. The degree of EUS phasic activity (bursting) during voiding was highly variable, with an average of 25% of voids not exhibiting bursting. Electrode implantation adjacent to the EUS yielded stable EMG recordings over extended periods and eliminated the confounding effects of anesthesia, physical restraint, and the potential for dislodgment of the chronically implanted intramuscular electrodes. These results show that micturition in unanesthetized, unrestrained rats is usually, but not always, associated with EUS bursting. This methodology is applicable to studying EUS behavior during progression of gradually evolving disease and injury models and in response to therapeutic interventions.

electromyography; chronic recording; implanted electrodes; longitudinal study; lower urinary tract

THE EXTERNAL URETHRAL SPHINCTER (EUS) muscle performs the vital function of regulating the timely passage of urine through the urethra (3, 17, 39). Abnormalities of lower urinary tract (LUT) function are common complications of chronic spinal cord injury, often arising from improper coordination of the EUS and detrusor muscles (4, 20). EUS dysfunction after injury or disease represents a serious health problem and is detrimental to the quality of life (1, 34, 40). Thus the complex neural control of the EUS and other muscles of the LUT has been an area of intense study for many years.

Studies of LUT function in animals typically employ recording of EUS electromyographic activity (EMG) using fine-wire electrodes inserted in the EUS muscle, often accompanied by bladder cystometry (2). The invasive nature of these techniques requires anesthesia or physical restraint to allow acquisition of

stable recordings of LUT function. Furthermore, because many of the disorders of LUT function involving the EUS develop gradually over time, using these acute methodologies to study changes in LUT function can be problematic; different groups of animals need to be studied at selected time points before or after application of the model perturbation (e.g., spinal contusion, bladder obstruction). The long-term nature of the health problems associated with EUS dysfunction would benefit from the availability of implantable intramuscular electrodes that would allow longitudinal study of EUS function over weeks and months. However, the EUS does not lend itself to long-term implantation with intramuscular electrodes. The sheet of EUS muscle that encircles the urethra is thin in the female rat (~0.2 mm) (13), which has become a common model for study of LUT function; its anatomy renders it prone to wire dislodgment and/or muscle damage due to body movement that applies forces to the wires that can pull them out of position during the long period of implantation.

The lack of methodology for chronic intramuscular recording of EUS activity has made long-term study of this aspect of LUT function difficult. In the present study, our aim was to develop methods for chronic study of EUS EMG in unanesthetized, unrestrained rats. To accomplish this, we surgically implanted rats with fine wires fixed to the pubic bone adjacent to the EUS to record its EMG; wires were routed subcutaneously to a plug attached to the skull, which connected to a removable flexible cable and a commutator to allow signal transmission to recording equipment while the animal moved freely in its cage. Preliminary reports of some of these data have appeared in abstract form (6, 22, 21).

MATERIALS AND METHODS

Animals

Subjects were 23 female Sprague-Dawley rats (8–12 wk old at time of entry into the study), housed individually with a 12:12-h light-dark cycle. All animal procedures were in accord with the *Guide for the Care and Use of Laboratory Animals* of the Institute of Laboratory Animal Resources, Commission on Life Sciences, National Research Council (National Academy Press, Washington, DC, 2010) and had been reviewed and approved by the Wadsworth Center Institutional Animal Care and Use Committee.

Implant Construction

Fine stainless steel multistranded wires (AS828 or AS631, Cooner Wire, Chatsworth, CA) were stripped of 4 mm of their Teflon insulation at one end. Each stripped wire end was twisted by the end of the wire being held with fine forceps while the rest of the wire was manually spun between finger and thumb, which served to stiffen and prevent fraying of the multistranded wire. The final 2 mm of one twisted end of each wire was folded down, and the entire stripped end

Address for reprint requests and other correspondence: J. S. Carp, Wadsworth Center, New York State Dept. of Health, PO Box 509, Albany, NY 12201 (e-mail: carpj@wadsworth.org).

was inserted into a connector pin (E363/0, Plastics One, Roanoke, VA), crimped, and soldered. Each pin was coated with a biocompatible sealant (Silicone Medical Adhesive, Dow-Corning, Midland, MI) and inserted into a 6.9 mm (h) \times 7.7-mm (d) plastic pedestal (MS363, Plastics One). A 2-cm length of silicone tubing (0.64 mm od \times 0.30-mm id Silastic, Dow-Corning) was threaded over each wire's free end and advanced until it reached the end soldered into the pins in the pedestal. The wires with their protective tubing were bent 90° just before entering the pins to exit the pedestal perpendicularly. The exposed pins, solder joints, wires, and the first few millimeters of protective tubing were encased in epoxy. A completed pedestal is shown in Fig. 1A.

EMG electrodes were formed from the free end of the pedestal wires. In the initial design used in the first two animals, the final 2 mm were simply deinsulated and twisted as described above. The final, more robust design was used in the subsequent four animals. First, the free end of each wire was stripped of 4 mm of insulation, twisted, and its final 2 mm folded back on itself. A small hook was inserted into the bend in the wire and rotated while the pair of bare wires was grasped near the end of the insulation with forceps, which twisted bare wire segments together with a small loop (\sim 0.25–0.3 mm od) at the top (Fig. 1B). The twisted wire segments were secured with a small drop of epoxy near the end of the insulation to prevent unraveling. Grounding wires were formed by deinsulation of the final 2 mm of the pedestal wires, twisting them as described above, and bending the stripped ends into a hook.

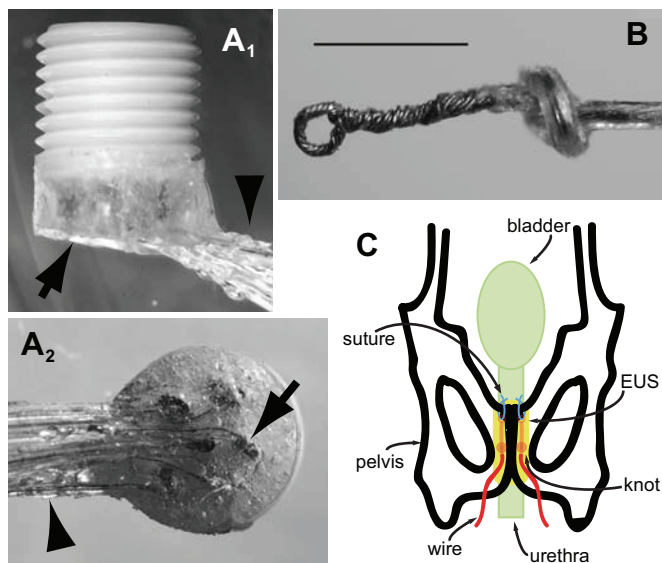


Fig. 1. Electrode construction and implantation. *A*: connector pedestal for mounting on the skull. A side view (*A1*) shows the pedestal oriented with its threaded plastic body pointing up for accepting the cable that connects to recording equipment via a commutator and electrode wires protected by epoxy (arrow) and silicone tubing (arrowhead) exiting from the base of the pedestal. A bottom view (*A2*) shows the part of the pedestal to be mounted onto the skull. Connector pins (one indicated by arrow) with electrode wires exiting tangentially are visible through the epoxy that protects and insulates them. The wires exit the epoxy through silicone rubber tubes (arrowhead) and are held together in a bundle with silicone adhesive. Pedestal diameter is 7.7 mm. *B*: electrode for implantation has a small loop twisted into its tip to allow it to be secured to the pubic bone with a suture. Calibration bar is 1 mm. *C*: diagram showing final position of external urethral sphincter (EUS) electromyographic (EMG) electrodes. Each electrode is passed across the pubic bone through a small hole and pushed rostrally until the loop end of the electrode emerges from under the rostral edge of the pubic bone. After securing of the loop end of the electrode to a second hole at the rostral edge of the pubic bone with a suture, the rest of the electrode wire is retracted through the caudal hole in the pubic bone to straighten the electrode into a position parallel and just lateral to the midline of the underlying urethra and EUS muscle.

Surgery for Implant Placement

All procedures were performed using sterile surgical techniques. Once rats were anesthetized with isoflurane (4–5% for induction, 1.5–2.5% for maintenance), two skin incisions were made, one mid-sagittal over the skull and one midline over the abdomen. The implant wires were inserted into a stainless steel tube with a point at the leading end. The tube was then passed subcutaneously from the skull incision to the abdomen, where it was externalized. The tube itself was pulled out through the abdominal incision, leaving the implant wires in the subcutaneous track with their free ends temporarily externalized for manipulation during the surgery. Blunt midline dissection through the rectus sheath and rectus abdominis muscle exposed the pubic bone. To position the two electrodes adjacent to the EUS, two bilateral holes were drilled manually with a 27-gauge needle in the pubic bone, each \sim 5 mm caudal to the rostral pubic bone edge and 0.5–1 mm lateral to the pubic symphysis. The EUS EMG wires were inserted through the holes into the ventral pelvic cavity. An overhand knot in each wire was tied just proximal to the bare ends. The wires were then retracted through the holes until the knot was pulled against the inside surface of the pubic bone, which prevented the wires from slipping back through the holes.

To position the EMG electrodes, a second pair of holes was drilled 1 mm caudal to the rostral pubic bone edge and 0.5–1 mm lateral to the pubic symphysis. On each side, a short length of 5-0 nylon suture was passed through the hole and the loop at the electrode tip, and then tied, securing the electrode end to the bone. This positioning is illustrated in Fig. 1C. One or two grounding wires were positioned subcutaneously either over the lower vertebral column or within the abdominal cavity.

In four animals, an additional pair of EMG electrodes (2-mm straight tip, twisted, no loop) were implanted in the pubocaudalis muscle on one side. The wires were bent into a hook and inserted with a 30-gauge needle from the pelvic cavity into the muscle under the pubic bone. To provide strain relief, a 3-cm length of wire was coiled into the pelvic cavity and then secured with 5-0 nylon suture to a hole drilled with a 27-gauge needle in the edge of the pubic bone \sim 3 mm rostral to the pubic symphysis. In another animal, an additional pair of EMG electrodes (2-mm straight tip, twisted, no loop) was implanted in the rectus abdominis muscle just rostral to the pubic bone. The wires were bent into a hook and inserted with a 30-gauge needle, and were strain relieved by suturing a 3-cm coil of wire to adjacent connective tissue.

About 3–4 cm of the insulated wires from the EUS and pubocaudalis EMG electrodes were looped within the abdominal cavity. The abdominal wall and abdominal skin incisions were closed in layers with absorbable suture (6-0 PDS II and 5-0 Vicryl or Vicryl Rapide, respectively). The animal was then turned to the prone position, and its head was secured in a stereotaxic frame. Four screws (00–96 \times 3/32 in.) were inserted into four holes drilled in the skull. The pedestal containing the connector pins was centered between the four screws with wires against the skull. The base of the pedestal and the four exposed screws were then covered with dental cement to secure the pedestal to the skull. All incisions were infiltrated with local anesthetic (bupivacaine), and topical antibiotic ointment (nitrofurazone) was applied to them after closure.

For 5–10 days after surgery, animals received antibiotics (gentamicin, 4 mg/kg ip twice daily and penicillin, 50,000 U/kg ip every other day) and an analgesic (carprofen; 10 mg/kg sc immediately after surgery, and 5 mg/kg sc twice daily subsequently).

Chronic Recordings

All 23 animals received chronic EUS EMG electrode implants; of these, six were used for long-term (\geq 8 wk) study, one of which failed after 3 wk due to electrode wire breakage. The other 17 rats were studied for 1–6 wk (median = 3 wk) before being entered into other studies.

EUS EMG and urine weight recording sessions began no sooner than 1 wk after surgery and continued at a rate of 1–3/wk for up to 14 wk. During each recording session, rats were housed individually for 24 h in a metabolic cage (Tecniplast, West Chester, PA) modified by replacing the stock lid with a conical cover to increase the internal vertical dimension of the cage. A flexible armored cable attached to the pedestal mounted on the rat's skull connected the implanted wires to recording equipment via a commutator. This permitted the rat to move freely about its cage during the recording session. The wire grid floor of the metabolic cage allowed urine to fall into funnels that diverted feces into a waste cup and urine into a collection cup mounted on a force transducer (FT03, Grass Technologies, Warwick, RI) that weighed the accumulating urine. The minimum delay between void onset and its detection at the force transducer due to drop transit time along the metabolic cage funnels was 0.62 s. The bottom of the force transducer cantilever arm was attached to a plastic float immersed in mineral oil to dampen oscillations in the urine weight recording due to drop arrival or vibrations external to the cage. A small quantity of mineral oil in the urine collection cup prevented evaporation of the accumulating urine. EMG and force transducer signals were routed from the commutator to the recording apparatus in an adjacent room.

Acute Recordings

After completing the chronic recordings, four of the implanted rats were anesthetized with a mixture of ketamine (80 mg/kg) and xylazine (10 mg/kg) for acute terminal experiments. Animals were maintained on a 37°C surgical platform during surgery and subsequent recordings while heart rate, respiratory rate, and blood oxygen saturation were monitored (MouseOx, Starr Life Sciences, Oakmont, PA). In one rat, an additional pair of wires for recording EUS EMG was inserted with fine-gauge needles alongside the urethra using a perineal approach for comparison with the EMG recorded from the chronically implanted electrodes. A fluid-filled catheter was inserted through the urethra into the bladder to record bladder pressure and deliver saline. EUS EMG and bladder pressure were recorded as a constant saline infusion (0.2 ml/min) into the bladder stimulated micturition reflexes.

In two rats, the pudendal nerve was dissected free from surrounding tissue for nerve stimulation. A dorsal skin incision was made parallel to the vertebral column extending from the iliosacral junction to the anterior aspect of the ileum. The underlying muscles were cut and reflected to expose the sacral plexus and ischioanal fossa. The iliosacral junction was gently separated to allow access to the ischioanal fossa and pudendal nerve. The motor branch of the pudendal nerve was placed on a bipolar hook electrode and covered with warm mineral oil for electrical stimulation.

Data Acquisition and Analysis

In the first two rats, the EMG data were band-pass filtered (35–100 Hz), full-wave rectified, and low-pass filtered again (32 Hz), digitized at 200 Hz, and stored. In the subsequent 21 rats, EMG data were band-pass filtered (10–300 Hz), digitized at 600 Hz, full-wave rectified digitally, downsampled to 200 Hz, and stored. Urine weight recordings were low-pass filtered (12 Hz) to further remove oscillations from the signal. During acute recordings, EUS EMG data were band-pass filtered (10–1,000 Hz), and bladder pressure data were low-pass filtered (1,000 Hz); all data were digitized at 2,000 Hz and stored.

EMG and urine weight data were analyzed using custom-designed software (Igor Pro, Wavemetrics, Lake Oswego, OR). Power spectra of EMG signals were obtained using the fast Fourier transform (FFT) algorithm. Time-frequency spectrograms were obtained by repeating FFT computations every 0.1 s on overlapping 1-s epochs of Hanning-windowed EMG data, with a $\times 0.1$ scaling factor applied to correct for this overlap and a $\times 1/0.375$ factor applied to compensate for power loss due to windowing.

Although data were collected throughout each 24-h session, analysis focused on episodes of voiding. Void onset was determined by a urine weight increase of at least 0.04 g. The bulk of the urine flow during a void typically consisted of a series of closely spaced drops (Fig. 2A). In these cases, void duration was determined by the time between registration of the first and last drop. For voids containing late-falling drops (empirically determined to be drops delayed by at least 0.8 s from the preceding drop and falling up to 120 s after void onset), the initial rate of urine accumulation was extrapolated to include late falling drops as if the total void volume accumulated in a single bolus (Fig. 2B). Thus the void duration reflects the time during which urine accumulated but ignores intravoid pauses in flow.

Determination of EUS EMG properties during voiding was based on the onset and offset of urine accumulation (as determined above) and the pattern of EUS EMG. Previous studies of micturition in anesthetized rats found that increased tonic EUS EMG accompanied the onset of bladder contraction (guarding reflex) and then transitioned into a phasic activation pattern during voiding (19, 38). In the present study, EUS guarding was evident before almost all voids (e.g., Fig. 2, A and B), but the degree of subsequent phasic activity was highly variable, ranging from robust bursting (Fig. 2A) to a completely tonic pattern (Fig. 2B; see *EMG Recordings* in RESULTS and Fig. 8 for further analysis and illustration of bursting variability). Because EUS bursting was not consistently evident during voiding, it could not be used to identify the transition from guarding to voiding. Instead, an empirical approach was used to define this transition point using spectral analysis of voids with visually identified bursting. Figure 3A shows spectral power (expressed as % total power) of 1-s epochs of EUS EMG just before (dashed line) and just after (solid line) bursting onset (average of each animal's average spectrum). Power changed significantly during the transition from guarding to voiding (indicated by asterisks in Fig. 3A for $P < 0.05$ by paired *t*-test). A similar analysis in individual animals (Fig. 3B) shows that power significantly decreases from guarding to voiding at 2 Hz (20/23 animals), 11–12 Hz (13/23 animals), and 21–30 Hz (16/23 animals); no animal showed significant increases in power at these frequencies. Significant increases or decreases in power were detected in other frequency bands in many animals, but these were accompanied by significant changes in power in the opposite direction in other animals [e.g., in the 4–9-Hz range (presumably reflecting EUS bursting), power increased in 16/23 animals, but decreased in 4/23 animals]. Based on the most consistent findings, a composite of EUS EMG power at 2, 11–12, and 21–30 Hz (P_{trans}) was calculated for identifying the transition from guarding to voiding in all voids, regardless of the presence or absence of bursting (*bottom* traces in Fig. 2, A and B, respectively). We defined the transition from guarding to voiding as the point on the falling phase of the P_{trans} before the urine accumulation onset plus 0.62 s (to account for the urine measurement delay) that exhibited the maximum rate of decrease in P_{trans} . Void offset was calculated as the sum of the void EMG onset and urine accumulation duration.

The following void-associated EMG properties were calculated between void EMG onset and void EMG offset: average EMG amplitude; bursting power (P_{burst}), defined as the average signal power in the EUS bursting-frequency range (4–10 Hz in 22 rats and 3–9 Hz in 1 rat) expressed as a percentage of the total average power; bursting time, defined as the cumulative time during which the bursting power was above a threshold value, defined as the mean P_{burst} in amplitude-matched non-voiding epochs plus $2 \times$ its SD; and dominant frequency, defined as the average of the frequencies with the highest power from all spectra calculated during the void with non-zero bursting time.

Post Mortem Assessments

During necropsy after euthanasia, the pubic bone was carefully removed and the location and integrity of the recording electrode

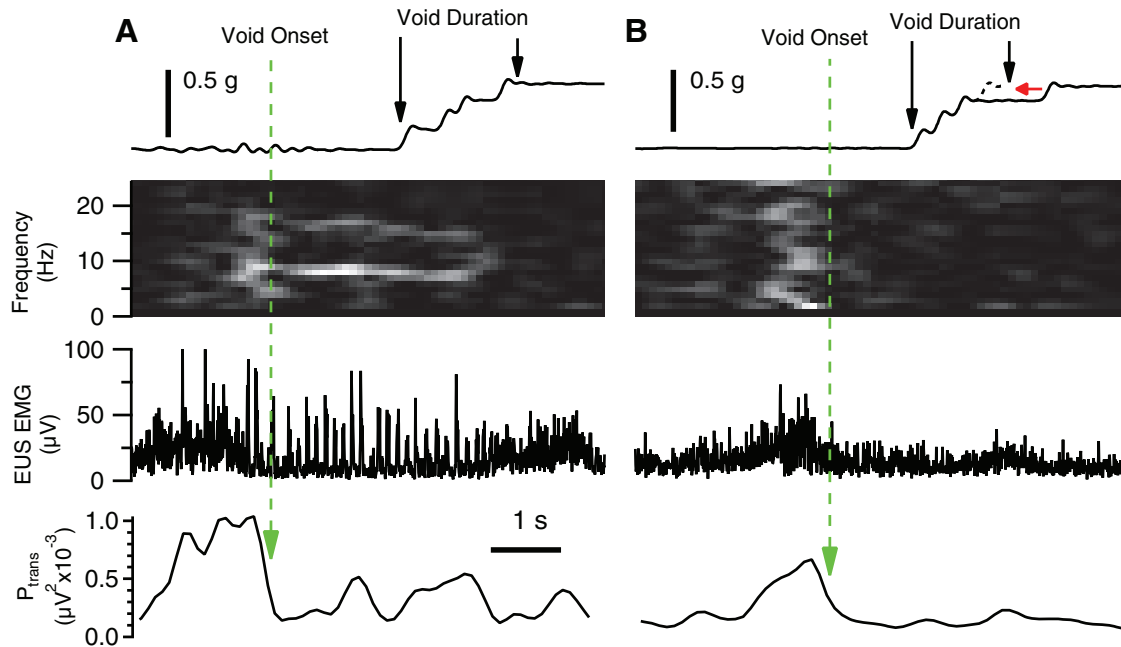


Fig. 2. Identification of micturition timing parameters in voids with different amounts of EUS bursting. *A*: void duration of a continuous urine bolus (*top* trace) is the time between the urine accumulation onset and offset (*left* and *right* vertical arrows, respectively). The sum of EUS EMG power at 2, 11–12, and 21–30 Hz (P_{trans}) is calculated for identifying the transition from guarding to voiding in all voids (*bottom* trace; see *Data Acquisition and Analysis* in MATERIALS AND METHODS for details). Void onset (long-dashed vertical arrow) is defined as the time of maximum rate of decrease in P_{trans} before urine accumulation onset plus 0.62 s (to account for the minimum urine measurement delay). In this example, EUS EMG exhibits bursting during the void (second panel from the *bottom*), which is evident in the time-frequency spectrogram as a bright band at ~7–9 Hz (second panel from the *top*). Void EMG offset is defined as void EMG onset plus void duration. *B*: void duration with incomplete initial urine bolus (delayed drop indicated by arrowhead in *top* trace) is determined by the time between the urine accumulation onset and the estimated urine accumulation offset (*left* and *right* vertical arrows, respectively), calculated as the time of intersection of the extrapolated rate of urine accumulation (short-dashed diagonal line) and the final level of accumulated urine weight (horizontal arrow). Void EMG onset (vertical long-dashed line) is determined as in *A* as the time of maximum rate of decrease in P_{trans} (*bottom* panel) before urine accumulation onset plus 0.62 s (long-dashed vertical arrow). Although the peak in P_{trans} before voiding is smaller than that observed for the void in *A*, their configurations are similar, and are both capable of identifying the transition from continence to voiding. Although there is no bursting evident [i.e., no bright band between 3 and 10 Hz in the spectrogram (second trace from *top*)], the void size is similar to the example shown in *A*, which exhibited robust bursting. Void EMG offset is defined as void EMG onset plus void duration.

wires were determined. In four of the five implanted animals recorded for ≥ 8 wk (and in 10 control animals without implants), the bladders were removed, emptied, cleaned, and weighed.

Statistics

Evaluations of urinary and EUS EMG properties over time were performed by ANOVA with repeated measures. Comparisons of urinary and EUS EMG properties between light and dark conditions were performed by paired *t*-test. EUS EMG spectral power before and after the transition from guarding to voiding were compared by paired *t*-test at each frequency.

RESULTS

Animal and Implant State

All animals recovered from surgery without incident. They resumed normal activity and food consumption within the next 1–2 days, and subsequently gained weight steadily (for the 5 rats studied for at least 8 wk, the average increase from surgery weight to *postoperative week 8* = 38 ± 11 g). Recording wires remained securely beneath the skin.

At the end of each experiment, necropsy confirmed that the EMG electrodes remained securely fixed with sutures intact in their original positions adjacent to the ventral surface of the EUS. Wires coiled within the abdominal cavity and routed subcutaneously to the skull-mounted pedestal were typically

ensheathed in connective tissue. The bladder and urethra appeared grossly normal. Average bladder weight was 62 ± 2 mg/200 g body wt, which was comparable to that seen in unimplanted rats (59 ± 3 mg/200 g body wt).

Urine Output

Figure 4A shows the time course of urinary parameters in the five rats studied over 8 wk of postimplantation study. Void weight, daily urine weight, number of voids, and void duration recorded throughout this study were not significantly different ($P > 0.05$ by ANOVA with repeated measures), indicating that these urinary parameters were stable over the 8 wk of recording.

During each 24-h recording session, urine weight increased in a series of steps formed by sequential voids, as illustrated for one session in Fig. 5 (*top* trace). In this trace, smaller, more frequent voids occurred during the 12-h dark period than during the 12-h light period. Figure 6A shows the average within-day time course of voiding properties for all rats. Rats exhibited diurnal variation in voiding, in that they produced significantly more voids at shorter intervoid intervals but of lesser weight during the dark period than during the light (Table 1). Also, total urine output was lower in the light than in the dark, suggesting that the higher void size in the light was

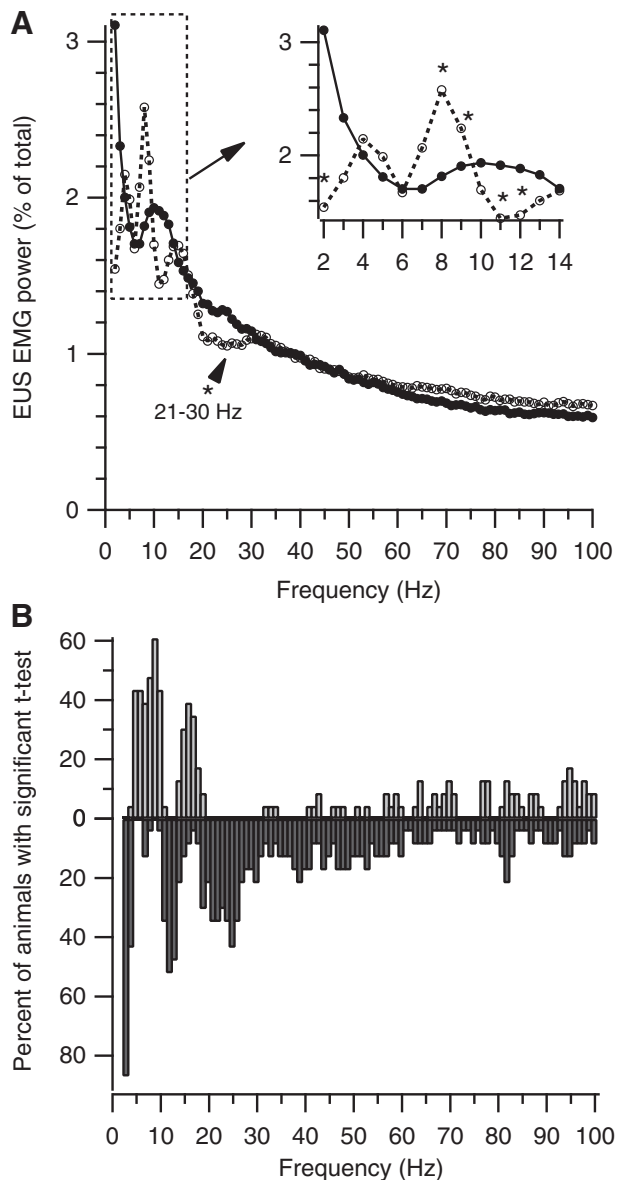


Fig. 3. Spectral analysis of transition from continence to voiding. *A*: average of average spectrum from each animal of 1 s of EUS EMG just before (● with solid line) and just after (○ with dashed line) the onset of EUS bursting. The dashed box indicates the area of enlargement shown in the inset in the top right corner. The transition from continence to voiding is associated with decreased power at 2, 11–12, and 21–30 Hz and with increased power at 8–9 Hz ($P < 0.05$ by paired t -test at each frequency). *B*: Percent of animals with significant difference between their average pre-voiding and voiding spectra ($P < 0.05$ by paired t -test) at each frequency. Upward and downward bars show significant increases or decreases, respectively, in power from pre-voiding to voiding.

not sufficient to balance the reduction in void frequency in that condition.

EMG Recordings

Previous studies of rat EUS EMG during micturition in anesthetized rats have reported characteristic phasic activation of the EUS muscle (bursting) in which short periods of increased amplitude EMG rapidly alternate with periods of EMG silence at rates of 3–10 Hz (19, 20, 38, 24, 28). We used spectral analysis to identify and quantify EUS bursting during

voiding. In the example shown in Fig. 2*A*, the time-frequency spectrogram (second panel from the top) exhibits a pronounced power band in the 7- to 9-Hz range that corresponds to the duration of EUS bursting. Figure 7 shows average spectra calculated for each animal during voiding (solid line) and non-voiding [long-dashed line; non-voiding spectra were calculated from 2-s epochs of EUS EMG that had average EMG amplitude matched to that of void EMG and that were at least 60 s before or after a void; $n = 453$ –110,413 epochs/animal (median = 35,907)]. The voiding spectrum contains peaks at 4, 8, and 15 Hz that are not present in the non-voiding spectrum. The difference in power at the lower two peaks presumably reflects the contribution of EUS bursting during voiding; the origin of the 15-Hz peak is not clear but may reflect, at least in part, an harmonic of the bursting-related peaks. These peaks were present in the spectra of almost every individual animal; 19 of 23 had a local maximum in the lower end of the bursting range (5, 13, and 1 rats at 3, 4, and 5 Hz, respectively), and 22 of 23 had a local maximum in the upper end of the bursting range (3, 7, 10, and 2 rats at 7, 8, 9, and 10 Hz, respectively). Of the 23 rats, 19 had peaks in both frequency ranges, 3 had only the peak in the 7- to 10-Hz range, and 1 had no clear peaks in either of the frequency ranges.

Although power in the bursting frequency range during voiding that exceeded the power in the same range during non-voiding EUS EMG epochs was found consistently from animal to animal, there was considerable variability in bursting within animals, and in the degree to which it was expressed. Figure 2*B* shows a void lacking clear evidence of bursting in the time domain EMG signal or in the frequency domain spectrogram, despite its being recorded ~ 2.5 h apart during the same session as and having a void size similar to that shown in Fig. 2*A*, where there is clear bursting. The range of inter- and intra-animal variability in EUS bursting during voiding is illustrated in Fig. 8 by pairs of EMG traces recorded from eight different animals (Fig. 8, *A–H*) during voids of comparable size with either a greater (top trace of pair) or lesser (bottom trace of pair) degree of EUS bursting. Many animals could produce voids of similar size either with or without robust bursting. Each EMG trace in this figure is associated with its void size (urine weight in grams) and bursting power (P_{burst}), calculated as the power in the bursting frequency range (typically 4–10 Hz; see MATERIALS AND METHODS) expressed as a percentage of the total power. The histograms below the EMG traces show the distributions in that animal of P_{burst} for all voids (solid line) and for 2-s non-voiding EMG epochs (dashed line). The mean value of the average P_{burst} in each animal was 14.8 and 6.1% for voiding and non-voiding epochs, respectively. There was considerable interanimal variability in P_{burst} during voiding (range: 8.5–31.8%) compared with P_{burst} in the absence of voiding (range: 4.8–7.9%). In addition, the distributions of P_{burst} for voiding and non-voiding epochs exhibited large variability in their degree of overlap. The % overlap was calculated as the percentile at which the voiding distribution had the same proportion of higher values of P_{burst} as the non-voiding distribution had of lower values of P_{burst} ; for example, in Fig. 8*A*, 88% of the values of P_{burst} during voiding exceeded 88% of the values of P_{burst} in the absence of voiding, i.e., a 12% overlap of the two distributions. The mean % overlap was $19.4 \pm 9.1\%$ (means \pm SD). The interanimal variation in % overlap was also high (range: 2–32%); while a

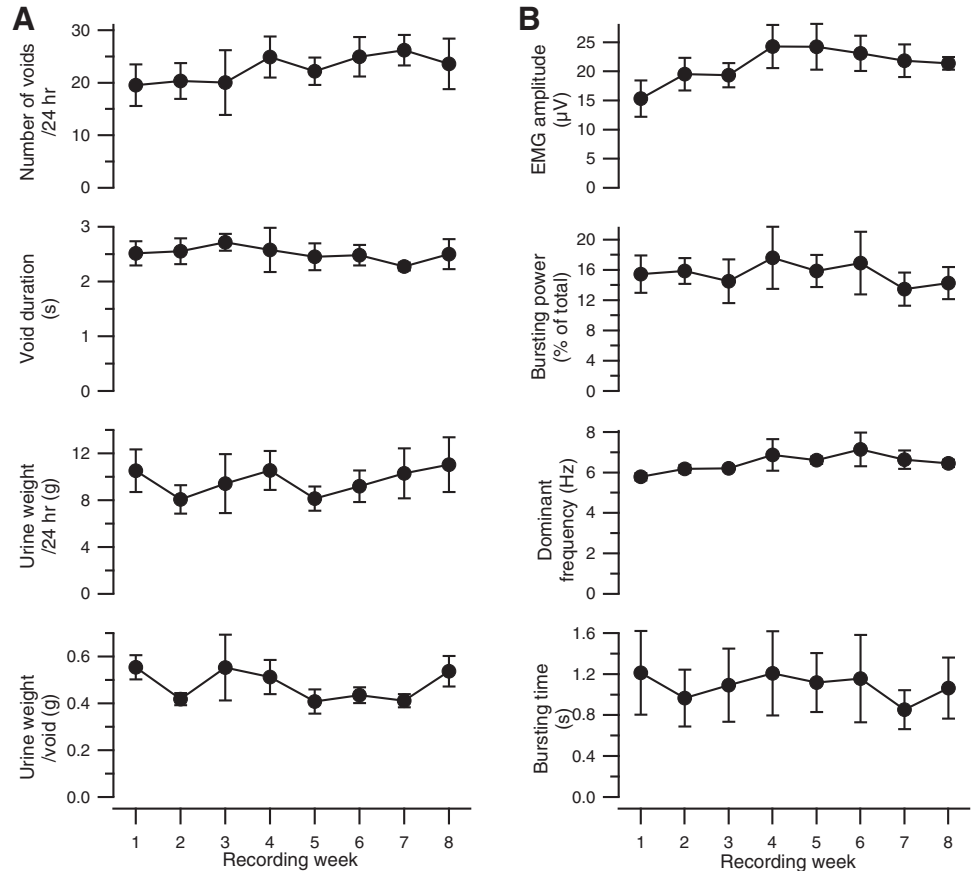


Fig. 4. Urine weight and EUS EMG data recorded from 5 rats over 8 wk. Weekly averages (\pm SE) of voiding (A) and EMG properties (B) are shown as a function of time after initial implantation. Urine weight/24 h, cumulative urine weight-200 g body wt⁻¹·24 h⁻¹; urine weight/void, urine weight-void⁻¹·200 g body wt⁻¹; EMG amplitude, average rectified EUS EMG amplitude during a void; bursting power, average power in bursting frequency range (typically 4–10 Hz) during a void expressed as percentage of total power during the same period of time; dominant frequency, average of frequency with highest power in bursting frequency range from all spectra during the void; bursting time, cumulative time during the void in which the bursting power exceeds the power in the bursting frequency range expressed as percentage of total power of amplitude-matched non-voiding epochs by 2 SD.

few animals exhibited bursting almost all the time (e.g., Fig. 8H), most animals exhibited a substantial number of voids in which EUS bursting (as assessed by P_{burst} and by visual inspection of the EMG traces) was modest or minimal.

The prevalence of voiding without EUS bursting was quantified as the number of voids with bursting time (as defined in MATERIALS AND METHODS) equal to zero. The percentage of voids

without bursting in individual animals was highly variable, ranging from 0 to 62% (Fig. 8I, left; means \pm SD, 25 \pm 19%). Many animals had a substantial number of nonbursting voids (e.g., 10 animals had at least 30% of their voids without bursting). This analysis is conservative in that it considers a void with any amount of bursting to be a “bursting void;” if voids with very brief bursting activity (e.g., \leq 0.2 s) are excluded, then the overall average percentage of non-bursting voiding increases to 35% (range for individual animals: 0–74%).

A large number of voids were associated with expulsion of small amounts of urine, e.g., 65% of voids weighed <0.5 g. Small voids typically have short durations, during which bursting may have been missed more often than in larger voids with longer durations, which theoretically could bias the results toward more apparent nonbursting voids. After these small voids were excluded, the findings were qualitatively similar to those based on the entire data set (Fig. 8I, right). On average across animals, voiding with no detectable bursting occurred 18% of the time, with the percentage of nonbursting voiding in individual animals ranging from 0 to 52%. Thus the expression of a substantial number of voids without bursting does not appear to be simply the result of the inclusion of a large number of small voids with brief bursting times.

Although voiding with little or no bursting appeared in many of the animals studied, it should be kept in mind that bursting was the most common pattern of EUS activity seen during voiding. In 20 of 23 animals, the majority of voids exhibited EUS bursting. Many animals showed consistent, near-exclu-

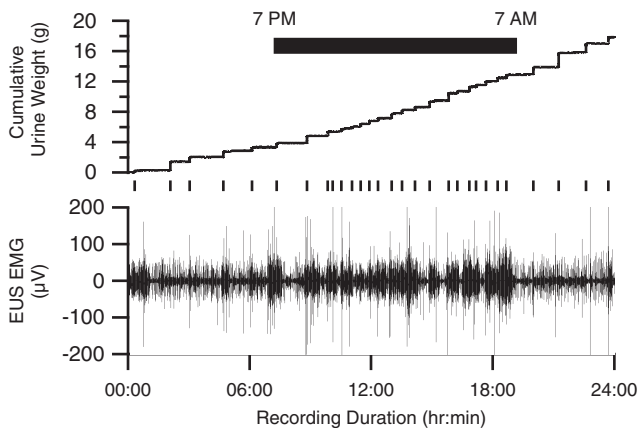


Fig. 5. Unrectified EUS EMG (bottom trace) and urine weight (top trace) acquired during one 24-h recording session. The raster plot below the urine weight trace identifies the timing of individual voids, which are evident as steplike increases in urine weight. Intervoid intervals were shorter and void weights were smaller during the 12-h period, when the room lights were turned off (black bar) and the rat was more active, than during the 12-h light period, when the rat was less active.

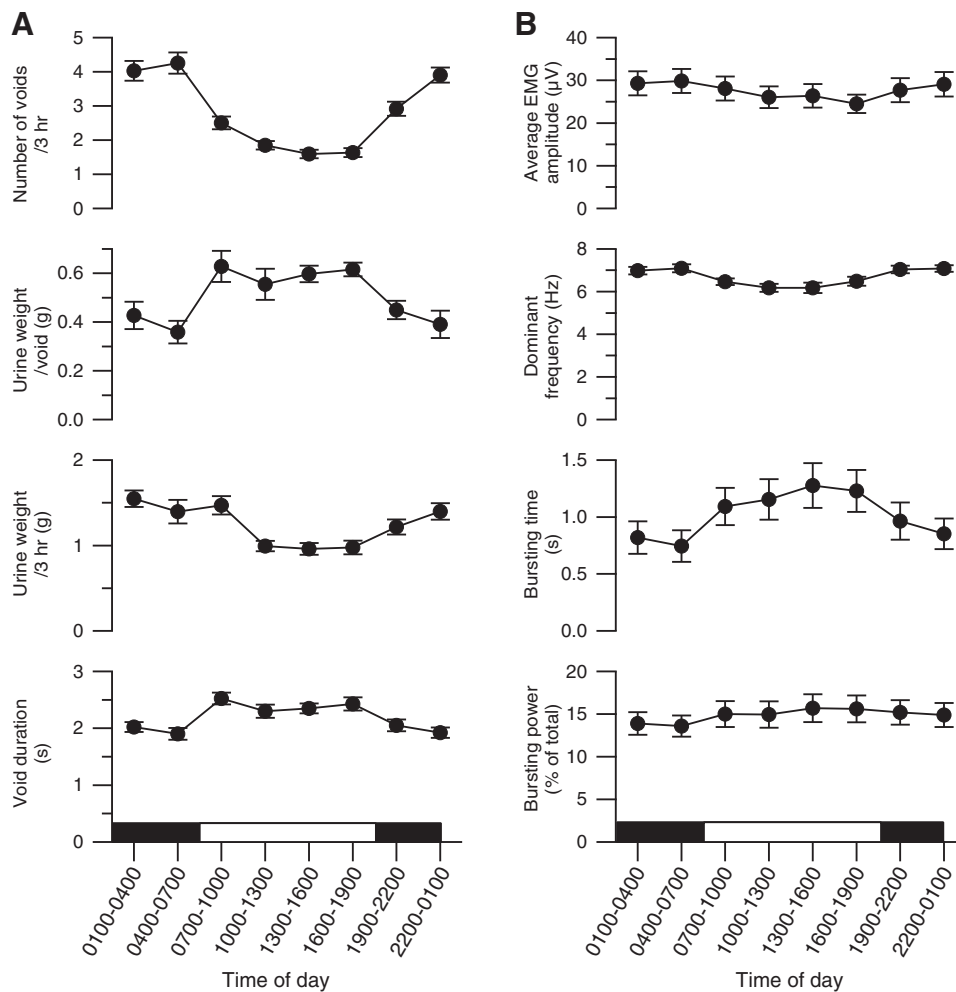


Fig. 6. Average diurnal variation in EUS EMG and voiding properties (\pm SE). EUS EMG and voiding properties are shown as a function of time of day (light-dark cycle indicated by the white and black horizontal bar). Urine weight/void, urine weight \cdot void $^{-1}$ \cdot 200 g body wt $^{-1}$; urine weight/3 h, cumulative urine weight per 200 g of body weight accumulated during each of the eight 3-h time periods; EMG amplitude, average rectified EUS EMG amplitude during a void; dominant frequency, average of frequency with highest power in bursting frequency range from all spectra during the void; bursting power, average power in bursting frequency range (typically 4–10 Hz) during a void expressed as percentage of total power during the same period of time; bursting time, cumulative time during the void in which the bursting power exceeds the power in the bursting frequency range expressed as percentage of total power of amplitude-matched non-voiding epochs by 2 SD.

sive bursting during voiding (e.g., 8 animals had fewer than 10% of their voids not associated with bursting). Thus bursting was the most common pattern of EUS activity observed during voiding in unanesthetized rats, but with considerable inter- and intra-animal variability in its expression. While EUS bursting is certainly an important feature of voiding in rats, its expression does not appear to be essential for spontaneous voiding to occur.

Figure 4B shows EUS EMG properties in the five rats recorded over at least 8 wk of postimplantation study. Average EUS EMG amplitude during the void varied significantly over this time ($P = 0.02$ by ANOVA with repeated measures). Average EUS EMG amplitude was significantly smaller during the first recording session (*week 1* in Fig. 3B) than during other weeks ($P < 0.05$ by multiple contrasts after ANOVA with repeated measures). After exclusion of the recordings from the

Table 1. EMG and urodynamic properties recorded during voiding in chronically implanted rats

Property	Daily	Dark	Light	P Value, Dark vs. Light ^a
Number of voids ^b	22.4 \pm 1.4	15.0 \pm 1.0	7.3 \pm 0.5	0.0001
Intervoid interval, s	75.5 \pm 4.1	56.2 \pm 3.4	99.9 \pm 5.6	0.0001
Daily urine output, g/200 g body wt ^c	9.8 \pm 0.6	5.5 \pm 0.4	4.2 \pm 0.3	0.0001
Urine output/void, g/200 g body wt	0.49 \pm 0.03	0.40 \pm 0.03	0.60 \pm 0.03	0.0001
Void duration, s	2.2 \pm 0.1	2.0 \pm 0.1	2.5 \pm 0.1	0.0001
EMG amplitude, μ V	28.6 \pm 2.7	29.9 \pm 2.8	28.5 \pm 2.7	0.002
Bursting power ^d , % of total	14.8 \pm 1.4	14.3 \pm 1.3	15.9 \pm 1.6	0.005
Bursting time ^e , s	0.93 \pm 0.14	0.82 \pm 0.14	1.16 \pm 0.17	0.001
Dominant frequency ^f , Hz	6.7 \pm 0.1	7.1 \pm 0.1	6.7 \pm 0.1	0.006

Values are means \pm SE. EMG, electromyography. ^aAnalysis by paired *t*-test within each animal for light vs. dark conditions. ^bNumber of voids per 24 h (daily) and per 12 h (dark, light). ^cCumulative urine weight per 24 h (daily) and per 12 h (dark, light). ^dAverage power in the bursting frequency range expressed as percent of average total power for all voiding events. ^eCumulative time during the void in which the bursting power exceeds the power in the same range, expressed as percentage of total power of amplitude-matched non-voiding epochs, by \pm 2 SD. ^fAverage frequency with highest power in bursting frequency range from all spectra calculated during the void.

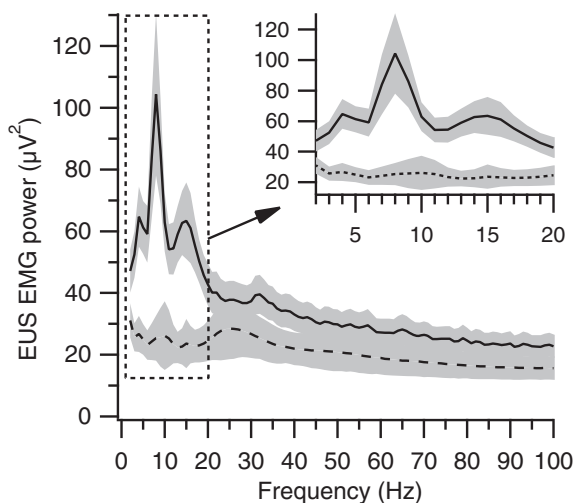


Fig. 7. Average of average spectra from each animal of EUS EMG during voiding (solid line) and during 2-s non-voiding (i.e., >60 s away from any voiding) epochs with average EMG amplitude matched to that observed during voiding. The gray bands around each spectrum delineate ± 1 SE. The dashed box indicates the area of enlargement shown in the inset in the top right corner. This region of the spectrum shows marked differences in power between voiding and non-voiding epochs at frequencies associated with EUS bursting (~ 3 – 10 Hz).

first recording session, there were no significant differences in void weight or any of the other urinary measurements ($P > 0.1$ for all by ANOVA with repeated measures) among the next 7 wk of recording (weeks 2–8 in Fig. 4B), indicating that voiding properties were stable during this time. An increase from the first to the second recording session was also found in the other rats with fewer than eight recording weeks (mean increase = $8.3 \pm 2.0 \mu\text{V}$, $P < 0.0001$ by paired t -test). Because the difference in the first session's responses may have reflected acclimation to the metabolic cage and/or recording cable, data from the first recording session from each rat were excluded from subsequent analyses.

Continuous recording of EUS EMG over 24-h periods also enabled detection of diurnal fluctuations (Fig. 6B). Rats exhibited significantly higher average EMG, smaller P_{burst} , shorter bursting time, and higher dominant bursting frequency during voiding in the dark than in the light part of the lighting cycle (Table 1).

Specificity of EMG Recordings

Many studies in anesthetized rats report that phasic EUS activation usually occurs during micturition (9, 13, 15, 38). Tonic EUS activity during micturition is associated with reduced voiding efficiency and is widely considered pathological because it is typically seen after injury in anesthetized rats (14, 16, 20, 23, 32). The finding that phasic EUS activation was not consistently detected in our normal unanesthetized rats was unexpected because a previous study of unanesthetized (but restrained) rats with intact neuraxes uniformly exhibited phasic EUS activity during micturition (23). This raised concern that the implanted EUS electrodes were not always recording reliably from the EUS muscle and/or that they were recording activity from nearby muscles.

The ability of the implanted electrodes to record from the EUS muscle was verified using two approaches. First, at the

end of this study, 16 of the 23 rats received midthoracic or upper-lumbar spinal transections. Subsequent chronic recording revealed clear EUS bursting during voiding in all 16 animals, even in 9 animals that displayed limited bursting in the spinally intact state (illustrated in Fig. 9A). This strongly indicates that the failure to detect EUS bursting in their earlier recordings with intact neuraxes was not due to the inability of the electrodes to record from the EUS muscle. In addition, we performed acute experiments under ketamine/xylazine anesthesia at the end of the chronic recordings in two other implanted rats to assess the recording specificity of the implanted electrodes. In one rat, saline infusion into the bladder through a urethral catheter elicited micturition reflexes (illustrated in Fig. 9B) characterized by strong phasic activation of the EUS muscle, even though this rat seldom exhibited robust phasic EUS activation during chronic (unanesthetized) recordings (average $P_{\text{burst}} = 11.6\%$ during voiding and 4.9% during non-voiding at matched average EMG amplitude). In addition, recordings from a pair of electrodes acutely implanted adjacent to the EUS using a perineal approach produced recordings that matched the temporal envelope of bursting (illustrated for 1 rat in Fig. 9B). Thus the chronic EUS electrodes used here were capable of recording bursting that matched that recorded using a standard acute electrode implantation methodology. In the second rat, EUS bursting accompanied spontaneous micturition reflexes. These observations support the validity of our finding that EUS bursting does not always occur during micturition in the awake, unrestrained rat.

To evaluate the issue of EMG cross talk, five rats with chronically implanted EUS electrodes were also implanted with electrodes in nearby muscles, pubocaudalis ($n = 4$), the nearest pelvic floor neighbor to the EUS muscle, and rectus abdominis ($n = 1$). EUS and pubocaudalis EMG signals correlated modestly throughout the day [average $r^2 = 0.15 \pm 0.05$ (means \pm SD)] for the correlation of an entire 24-h recording session from each rat). However, during voiding, EUS and pubocaudalis activity correlated much less [average $r^2 = 0.04 \pm 0.04$ (means \pm SD); illustrated in Fig. 9C]. EUS and rectus abdominis EMG signals were more weakly correlated throughout the day ($r^2 = 0.06$ for the correlation of an entire 24-h recording session) or during voiding ($r^2 = 0.00$). These data indicate that the EUS electrodes were recording little or no activity from the nearby pubocaudalis or rectus abdominis muscles (i.e., cross talk); they also suggest that the EUS and the other two muscles may have complementary activity during continence but have different roles during micturition.

Finally, these rats were subsequently anesthetized with ketamine/xylazine, and we stimulated the pudendal nerve, which innervates the EUS. Pudendal nerve stimulation ($2 \times$ threshold required to evoke a muscle response) elicited large compound muscle action potentials in the chronically implanted EUS electrodes and only small responses [peak-to-peak amplitude only $15 \pm 5\%$ (means \pm SD) of the EUS response] from electrodes implanted in pubocaudalis muscle (illustrated for 1 rat in Fig. 9D). These assessments of recording electrode specificity demonstrated that the EMG activity recorded from the electrodes chronically implanted adjacent to the EUS was produced almost entirely by the EUS muscle and that these electrodes provide a reliable assessment of EUS activation. Thus these results support the validity of the present finding

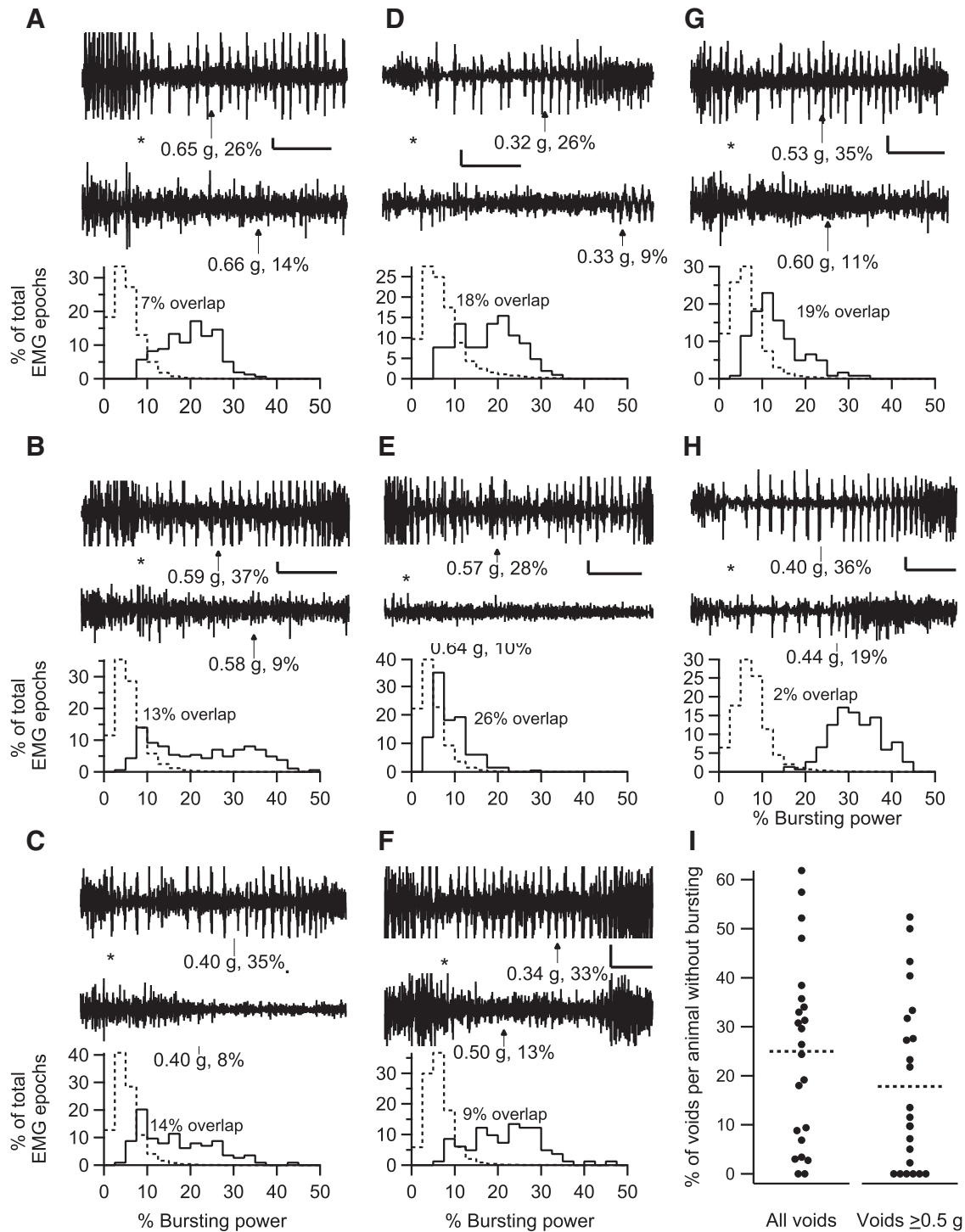


Fig. 8. Inter- and intra-animal variability in EUS bursting during voiding. *A–H*: data are shown from a different individual animal in each panel. The *top 2* traces show examples of EUS EMG that illustrate the range of EUS bursting in each animal during voids of comparable size (voided urine weights and average EUS EMG bursting power during the void are shown below each trace with an arrow pointing to the time of urine accumulation onset). The traces are aligned to the detected void onset (as illustrated in Fig. 2), which is indicated by the asterisk between the traces. In most animals, voids of similar size can occur with or without clear bursting (*A–G*), while 1 animal exhibited more consistent bursting (*H*). The histograms below the EMG traces show the distribution of power in the bursting range expressed as a percentage of total power during voiding (solid line) or during 2-s epochs of EUS EMG recorded under non-voiding conditions (i.e., ≥ 60 s away from any void; dashed line). There was overlap in the distribution of bursting power between voiding and non-voiding conditions, with considerable variation in the degree of overlap (% overlap indicated next to each pair of histograms). Time calibration bars for *A–H*: 1 s. EUS EMG voltage calibration: 100 μ V (*A*); 50 μ V (*B–E*, *G*, and *H*); 25 μ V (*F*). *I*: each marker (●) shows for each animal the percentage of voids that had no bursting (i.e., bursting time = 0, where bursting time is defined as the cumulative time during the void in which the bursting power exceeds the power in the bursting frequency range expressed as the percentage of total power of amplitude-matched non-voiding epochs by 2 SD). Data using voids of all sizes are shown on the *left*, and data using only voids ≥ 0.5 g are shown on the *right*. Some markers are offset slightly to the *left* or *right* to prevent overlap of data from animals with similar values. Mean values for each of the 2 groups of data are shown by dashed horizontal lines.

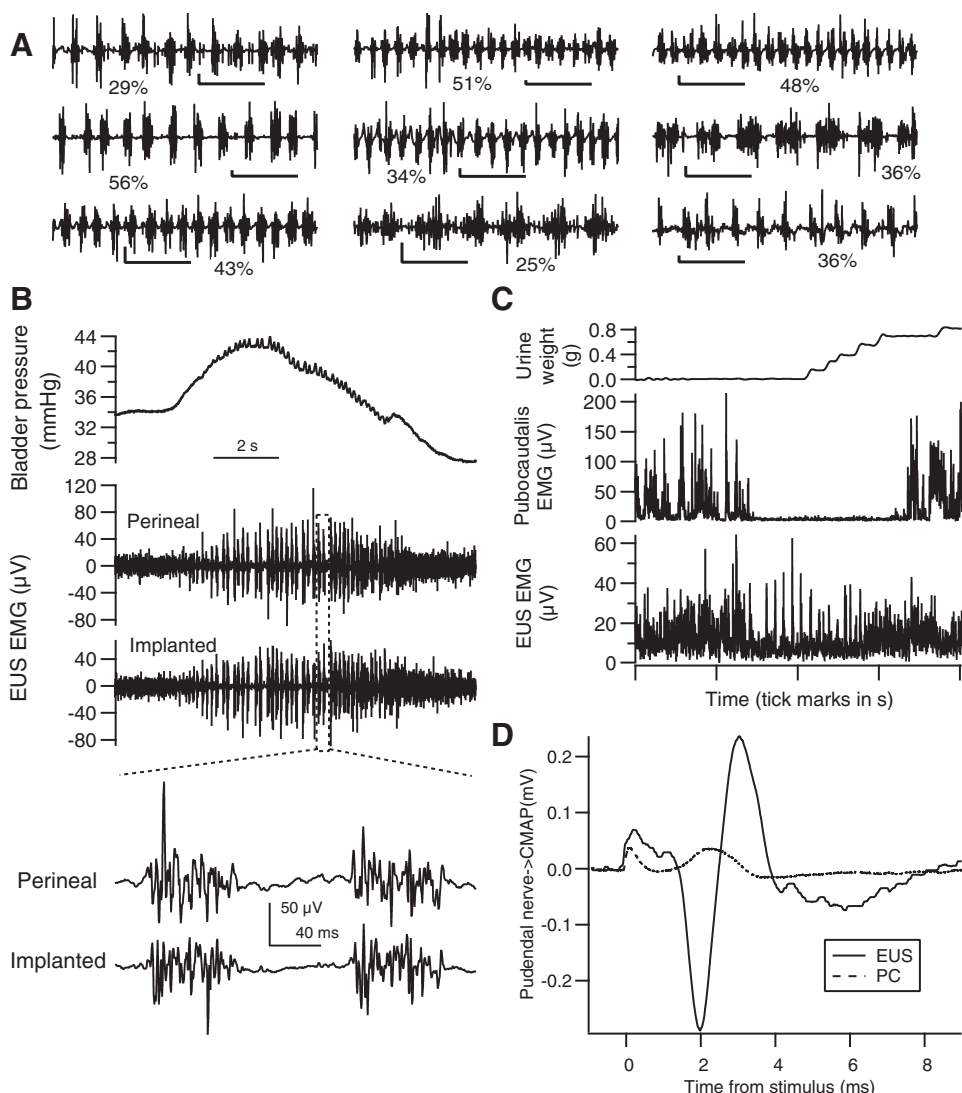


Fig. 9. Specificity of EUS recordings. *A*: EUS EMG recorded with the implanted electrodes in 9 of the unanesthetized rats used in the present study after receiving midthoracic or lower-thoracic/upper-lumbar spinal cord transections during voiding. Each of these rats had exhibited weak EUS bursting before transection (average % bursting power range: 8.5–10.4%); after transection, they showed strong bursting (% bursting power range: 25–56%; individual values shown adjacent to each trace), strongly suggesting that the electrodes would have been capable of recording bursting had it occurred during pretransection recordings. Calibration: 0.5 s, 30 μ V. *B*: bladder pressure and EUS EMG during cystometry in an acute experiment under ketamine/xylazine anesthesia from an implanted rat after completion of chronic recordings. Although phasic EUS EMG did not usually occur during voiding during chronic recording in this unanesthetized rat, bursting is clearly present in the anesthetized preparation, indicating that the implanted electrodes were properly located for recording from the EUS. A second pair of electrodes, inserted parallel but just lateral to the urethra using a perineal approach, shows similar bursting. The *inset* shows a magnified view of 2 cycles of bursting recorded from these electrodes. The EMG envelopes of the bursts in the 2 traces are similar although not identical, suggesting that the 2 electrode pairs are recording from different locations within the EUS. *C*: simultaneous recording of EUS and pubocaudalis muscles in an unanesthetized rat shows little or no correlation in EMG activity between the 2 muscles during voiding. *D*: compound muscle action potentials (CMAPs) recorded from electrodes chronically implanted adjacent to the EUS (solid line) and in the pubocaudalis muscle on one side (dashed line). Pudendal nerve stimulation elicits a large CMAP from the EUS electrodes, and only a small response from the pubocaudalis electrodes, implying that there is little cross talk between the EUS and pubocaudalis.

that micturition in the unanesthetized, unrestrained normal rat often occurs without EUS bursting.

DISCUSSION

Chronic EUS Recording Methodology

Development of chronic recording of EUS EMG activity in the unanesthetized, unrestrained rat has been hampered by the fact that this muscle does not lend itself to chronic implantation of intramuscular electrodes. The EUS has a thin cross-sectional profile and lacks the thick muscle belly and aponeuroses that

provide a firm hold and strong anchors for intramuscular electrode wires implanted in larger skeletal muscles. Thus we developed a novel method to implant in rats fine wires for chronic recording of EMG from this muscle. The key features of this method are 1) surgical fixation of the wire recording ends to bone to secure them adjacent to the ventral surface of the EUS; 2) subcutaneous routing of wires to a skull-mounted head pedestal; 3) electrical connection to the recording apparatus through a flexible cable and an electrical commutator; and 4) simultaneous collection of voided urine and recording of urine weight.

Surface electrodes may be more susceptible to nontarget sources. However, several observations make it unlikely that inadequate EMG amplitude or excessive cross talk from other muscles accounted for the variable, and in some cases quite modest, degree of EUS EMG bursting detected during voiding. First, during bladder cystometry in chronically implanted rats acutely anesthetized at the end of study, the chronically implanted electrodes detected strong EUS bursting during micturition reflexes, even in a rat in which strong bursting usually did not occur during micturition when the rat was not anesthetized. Second, implanted rats that showed variable bursting during micturition in the spinally intact state all showed consistent bursting after spinal transection. Third, pudendal nerve stimulation elicited EUS muscle activity that was detected by the implanted electrodes, providing further evidence that the EUS is the main contributor to the recorded EMG signal. Fourth, while EMG recorded from intramuscular electrodes in the pubocaudalis and rectus abdominis correlated modestly with EUS EMG during intervoid intervals, it correlated much less during voids. The variable degree of correlation between EUS and pubocaudalis or rectus abdominis in different conditions argues against the presence of proximity-based cross talk (which would be expected to be present during both continence and voiding). Lack of correlation between EUS and pubocaudalis EMG during voiding is consistent with the hypothesis that the pubocaudalis does not contribute to micturition in female rats (18), while modest intervoid correlations suggest related functionality during continence (25). Together, these findings indicate that the chronic fixation of electrodes adjacent to the ventral surface of the EUS enables them to record EUS EMG activity reliably while recording only a modest amount of activity from other muscles.

Advantages of Chronic EUS Recording Methodology

This new chronic EUS recording method does not require physical restraint or anesthesia, and thus it allows study of longitudinal and diurnal changes in EUS EMG activity during micturition and continence. This is important because anesthesia is known to alter rat micturition properties (5, 8, 10, 26, 41, 44). Furthermore, these methods permit recording of EUS EMG in awake, freely behaving animals. Surgical fixation of the strain-relieved wires to the pubic bone and subcutaneous routing of wires render them inaccessible to the rat and protect them from intentional and inadvertent damage and disruption. In the five rats in which long-term recording was performed, good recordings persisted over the course of the 8-wk experimental protocol (and well beyond that in several rats). After the first recording session, EMG and voiding properties were stable for the next 7 wk. The early variability may have reflected behavioral adjustments to the novel metabolic cage environment and/or recording apparatus, and possibly postsurgical tissue changes.

While physical restraint of animal subjects during urodynamic studies can mitigate or eliminate the influence of anesthesia on micturition properties, it is likely to produce physical and/or psychological stress (27, 31) which could influence micturition (30, 33, 35, 37). In this study, void size recorded during the first session after implantation differed from that in subsequent weeks (except in the 1 rat that had been previously exposed to the metabolic cage). This suggests that the first

exposure to the metabolic cage alone (or in combination with attachment of the flexible recording cable to the skull-mounted pedestal) influenced LUT function. Once the animals were adapted to the recording environment in which they were able to move about freely, their LUT function stabilized. Thus the new method described here permits repeated long-term assessment of LUT function in conditions that closely approximate the subjects' normal daily living conditions.

EUS Bursting During Voiding

In the present study, strong phasic activation of the EUS muscle did not always occur during micturition. This was surprising because EUS bursting is thought to be the dominant, if not the sole, pattern of EUS activation during micturition in rats with normal LUT function, and a mechanism for maximizing voiding efficiency in rats (9, 11, 13, 43). This raises the possibility that EUS bursting is not essential for voiding in the normal, unanesthetized unrestrained rat.

Previous studies of EUS activity in awake rats with intact neuraxes are rare due to the technical obstacles to recording EUS EMG and bladder pressure in awake animals. One study reported EUS bursting in 100% of unanesthetized, restrained rats with intact neuraxes during saline infusion into the bladder through a catheter acutely implanted through the bladder wall (23). These results may be attributable to the experimental conditions, in that a suprapubic catheter was implanted in the bladder and EUS EMG electrodes were implanted percutaneously via a perineal approach under isoflurane anesthesia, and then restrained, conscious cystometry was performed after discontinuance of isoflurane. Thus the EUS activation patterns observed during micturition in this study may have differed from those of the present study due to restraint-associated stress, tissue damage, and postsurgical pain due to acute surgical implantation, and saline infusion-evoked voiding (as opposed to physiological bladder filling-evoked spontaneous voiding).

Evidence for lack of or reduced EUS bursting during voiding in rats can be gleaned from other cystometric studies reported in unanesthetized rats. In unanesthetized, restrained female rats at least 1 wk after suprapubic bladder catheter implantation (12), most bladder contractions during cystometry were single peaks without the high-frequency pressure oscillations (HFOs; see Fig. 3 in Ref. 12) that are typically associated with EUS bursting; in urethane-anesthetized rats, bladder contractions exhibited both HFOs and EUS bursting (see Figs. 5 and 7D in Ref. 12). In another cystometric study performed in unanesthetized, freely moving rats (26), bladder pressure recordings during voiding shown in Fig. 1A in that study did not appear to exhibit HFOs; after administration of low-dose tiletamine-zolazepam anesthesia in the same animal, HFOs appeared to be present in the bladder pressure trace in Fig. 1B of that study; the apparent HFOs weakened and disappeared at progressively higher anesthetic doses (see Fig. 1, C and D, respectively, in Ref. 26). In a study using unanesthetized, decerebrate rats (44), there was no evidence of HFOs in bladder pressure recordings during cystometry (see Figs. 1 and 2 in that study). These observations are consistent with our findings that voiding can occur without EUS bursting in unanesthetized rats and that bursting emerges (or strengthens) under anesthesia.

Much of the literature describing studies of EUS muscle activity during micturition in rats with intact neuraxes used anesthesia or decerebration to eliminate pain and prevent disruption of recording by movement (15, 42, 44). These studies in anesthetized rats consistently report EUS bursting during micturition. Our results agree with these reports; strong EUS bursting emerged during both spontaneous and saline infusion-evoked voids in ketamine/xylazine-anesthetized rats.

The sensitivity to stress and anesthesia of EUS bursting during voiding suggests that supraspinal mechanisms partially suppress EUS bursting in the unanesthetized unrestrained normal rat. Complete removal of supraspinal inputs by spinal transection appears to restrict EUS activity during micturition in unanesthetized rats to the phasic pattern (22, 21). Thus the present data are consistent with the existence of a spinal pattern generator for bursting that is under supraspinal influence (7, 16).

An alternative explanation for the apparent lack of EUS bursting observed in this study is that bursting is indeed present in every void, but partial recruitment of the EUS motoneuron pool resulted in spatially heterogeneous EUS EMG activity that was sometimes missed by the implanted electrodes. While plausible, this seems unlikely given that in a study of EUS single-motor units, every unit tested was recruited during voiding (14).

Limitations of the Methodology

One limitation of this study is that it did not include a direct indicator of the contractile state of the urinary bladder. Knowledge of contractile activity and intravesical pressure of the bladder would provide context for EUS EMG during continence and would provide information on input from bladder afferents to spinal circuitry controlling the EUS. Measuring bladder activity is typically accomplished by suturing a small-diameter, fluid-filled catheter (in parallel with a pressure transducer) into the bladder to record pressure. However, chronic bladder cannulation is problematic because it can lead to infection, inflammation, and urolith formation, and catheters can easily occlude or dislodge (29, 41). In addition, cystometric instrumentation, such as bladder wall and transurethral catheterization, can affect micturition properties (36, 41). Thus it is generally desirable to study EUS activity and LUT function with minimal or no direct surgical damage to the soft tissues of the bladder. By securing the EMG electrodes to the dorsal surface of the pubic bone, just ventral to the urethra and the EUS, we recorded EUS activity without incising or penetrating the bladder, urethra, EUS, or other pelvic floor muscles.

A potential limitation of this method is that the electrodes recording EUS activity are surface electrodes. EUS muscle EMG is likely to be lower amplitude than EMG from intramuscular electrodes. Additionally, because the electrodes recording EUS activity were not in the EUS muscle, they may have been subject to more electrical cross talk from neighboring muscles. While the present results indicate that this was not a significant problem, it may be feasible to further reduce the possibility of cross talk in the future by placing insulation between the electrodes and other muscles.

Use of a metabolic cage permits urine collection without the need for restraint. At the same time, it introduces a small but variable delay in the arrival of the urine at the weighing station as the drops slide down the chamber walls. The delay is

typically ~ 0.6 – 2 s but can be longer if the urine drops encounter any impediments (e.g., food crumbs, feces). This uncertainty in the exact timing of the voided urine led us to develop a voiding-onset detector based on empirical evidence of a decrease in power in three frequency ranges, i.e., 2, 11–12, and 21–30 Hz, of the EUS EMG spectrum from just before and to just after void onset (as determined from voids in which EUS bursting was clearly visible). These specific frequencies are presumably sensitive to the transition from continence to voiding. A decrease in the 21- to 30-Hz power band may reflect the discontinuation of the EUS motor unit firing repetitively during the guarding reflex at void onset. In some animals (e.g., Fig. 7A), voiding is preceded by a brief period of bursting at frequencies of 11–15 Hz before transitioning to the lower range of frequencies (i.e., 3–10 Hz) more typically associated with voiding; the reduction in 11- to 12-Hz power may be a reflection of this transition. The cause of the decrease in power at 2 Hz is the least evident of the three frequency ranges, but it is possible that it reflects movement of the EUS muscle relative to the implanted electrode caused by voiding-associated changes in the urethra due to relaxation of its smooth muscle and/or changes in the bladder muscle contractile state. Dependence of identification of void onset on this empirical method could be avoided by development of a method for detecting urine production closer to its source.

Conclusions

The new methodology described here allows repeated recording of EUS muscle activity in unanesthetized, unrestrained rats over months. This methodology should be particularly useful for studies of EUS behavior and other aspects of LUT function during traumatic or disease processes that evolve gradually, such as the chronic phase of recovery from spinal injury. The practical value of this new method is illustrated by the finding that while micturition in awake, freely moving normal rats is typically associated with EUS bursting, it also occurs in a substantial number of cases with little or no EUS bursting activity. This finding contradicts the standard belief, based on recording in anesthetized or awake, restrained rats that EUS bursting always accompanies micturition. The value of this new method could be further enhanced by combining it with a new nontraumatic method for chronic monitoring of bladder activity.

ACKNOWLEDGMENTS

The authors thank Richard Cole of the Advanced Light Microscopy Core of the Wadsworth Center for assistance with image collection and preparation.

GRANTS

This study was supported by the Craig H. Neilsen Foundation (J. S. Carp), the National Institutes of Health (NS22189, J. R. Wolpaw; HD36020, X. Y. Chen; NS061823, J. R. Wolpaw and X. Y. Chen), and the New York State Spinal Cord Injury Trust Fund (X. Y. Chen).

DISCLOSURES

No conflicts of interest, financial or otherwise, are declared by the authors.

AUTHOR CONTRIBUTIONS

Author contributions: B.K.L., J.R.W., X.Y.C., and J.S.C. provided conception and design of research; B.K.L. and J.S.C. performed experiments; B.K.L. and J.S.C. analyzed data; B.K.L., J.R.W., X.Y.C., and J.S.C. interpreted results of experiments; B.K.L. and J.S.C. prepared figures; B.K.L. and J.S.C. drafted

manuscript; B.K.L., J.R.W., X.Y.C., and J.S.C. edited and revised manuscript; B.K.L., J.R.W., X.Y.C., and J.S.C. approved final version of manuscript.

REFERENCES

- Anderson KD. Targeting recovery: priorities of the spinal cord-injured population. *J Neurotrauma* 21: 1371–1383, 2004.
- Andersson KE, Soler R, Fullhase C. Rodent models for urodynamic investigation. *Neurourol Urodyn* 30: 636–646, 2011.
- Beckel JM, Holstege G. Neurophysiology of the lower urinary tract. *Handb Exp Pharmacol* 149–169, 2011.
- Blaivas JG, Sinha HP, Zayed AA, Labib KB. Detrusor-external sphincter dyssynergia: a detailed electromyographic study. *J Urol* 125: 545–548, 1981.
- Cannon TW, Damaser MS. Effects of anesthesia on cystometry and leak point pressure of the female rat. *Life Sci* 69: 1193–1202, 2001.
- Carp JS, LaPallo BK, Chen XY, Wolpaw JR. External urethral sphincter muscle activity and bladder length recorded in freely moving adult female rats: methods development. In: *Abstract Viewer and Itinerary Planner*. Washington, DC: Society for Neuroscience Online, Abstract 393.14, 2011.
- Chang HY, Cheng CL, Chen JJ, de Groat WC. Serotonergic drugs and spinal cord transections indicate that different spinal circuits are involved in external urethral sphincter activity in rats. *Am J Physiol Renal Physiol* 292: F1044–F1053, 2007.
- Chang HY, Havton LA. Differential effects of urethane and isoflurane on external urethral sphincter electromyography and cystometry in rats. *Am J Physiol Renal Physiol* 295: F1248–F1253, 2008.
- Chen SC, Lai CH, Fan WJ, Peng CW. Sex differences in the external urethral sphincter activity of rats. *J Exp Clin Med* 4: 157–164, 2012.
- Cheng CL, de Groat WC. The role of capsaicin-sensitive afferent fibers in the lower urinary tract dysfunction induced by chronic spinal cord injury in rats. *Exp Neurol* 187: 445–454, 2004.
- Conte B, Maggi CA, Parlani M, Lopez G, Manzini S, Giachetti A. Simultaneous recording of vesicle and urethral pressure in urethane-anesthetized rats: effect of neuromuscular blocking agents on the activity of the external urethral sphincter. *J Pharmacol Methods* 26: 161–171, 1991.
- Cruz Y, Downie JW. Abdominal muscle activity during voiding in female rats with normal or irritated bladder. *Am J Physiol Regul Integr Comp Physiol* 290: R1436–R1445, 2006.
- Cruz Y, Downie JW. Sexually dimorphic micturition in rats: relationship of perineal muscle activity to voiding pattern. *Am J Physiol Regul Integr Comp Physiol* 289: R1307–R1318, 2005.
- D'Amico SC, Collins WF 3rd. External urethral sphincter motor unit recruitment patterns during micturition in the spinally intact and transected adult rat. *J Neurophysiol* 108: 2554–2567, 2012.
- D'Amico SC, Schuster IP, Collins WF, 3rd. Quantification of external urethral sphincter and bladder activity during micturition in the intact and spinally transected adult rat. *Exp Neurol* 228: 59–68, 2011.
- Dolber PC, Gu B, Zhang X, Fraser MO, Thor KB, Reiter JP. Activation of the external urethral sphincter central pattern generator by a 5-HT_{1A} receptor agonist in rats with chronic spinal cord injury. *Am J Physiol Regul Integr Comp Physiol* 292: R1699–R1706, 2007.
- Fowler CJ, Griffiths D, de Groat WC. The neural control of micturition. *Nat Rev Neurosci* 9: 453–466, 2008.
- Jiang HH, Salcedo LB, Song B, Damaser MS. Pelvic floor muscles and the external urethral sphincter have different responses to applied bladder pressure during continence. *Urology* 75: e1511–e1517, 2010.
- Kakizaki H, Fraser MO, de Groat WC. Reflex pathways controlling urethral striated and smooth muscle function in the male rat. *Am J Physiol Regul Integr Comp Physiol* 272: R1647–R1656, 1997.
- Kruse MN, Belton AL, de Groat WC. Changes in bladder and external urethral sphincter function after spinal cord injury in the rat. *Am J Physiol Regul Integr Comp Physiol* 264: R1157–R1163, 1993.
- LaPallo BK, Carp JS, Chen XY, Wolpaw JR. Chronic recording of external urethral sphincter EMG and urine output before and after L1 spinal transection in female rats. In: *Abstract Viewer and Itinerary Planner*. Washington, DC: Society for Neuroscience Online, Abstract 657.17, 2013.
- LaPallo BK, Carp JS, Chen XY, Wolpaw JR. External urethral sphincter activity recorded during voiding in unanesthetized intact and spinal-transected rats. In: *Abstract Viewer and Itinerary Planner*. Washington, DC: Society for Neuroscience Online, Abstract 484.04, 2012.
- Leung PY, Johnson CS, Wrathall JR. Comparison of the effects of complete and incomplete spinal cord injury on lower urinary tract function as evaluated in unanesthetized rats. *Exp Neurol* 208: 80–91, 2007.
- Maggi CA, Giuliani S, Santicoli P, Meli A. Analysis of factors involved in determining urinary bladder voiding cycle in urethane-anesthetized rats. *Am J Physiol Regul Integr Comp Physiol* 251: R250–R257, 1986.
- Manzo J, Esquivel A, Hernandez ME, Carrillo P, Martinez-Gomez M, Pacheco P. The role of pubococcygeus muscle in urinary continence in the male rat. *J Urol* 157: 2402–2406, 1997.
- Matsuura S, Downie JW. Effect of anesthetics on reflex micturition in the chronic cannula-implanted rat. *Neurourol Urodyn* 19: 87–99, 2000.
- Matsuura T, Takimura R, Yamaguchi M, Ichinose M. Estimation of restraint stress in rats using salivary amylase activity. *J Physiol Sci* 62: 421–427, 2012.
- Mersdorf A, Schmidt RA, Tanagho EA. Urodynamic evaluation and electrical and pharmacologic neurostimulation. The rat model. *Urol Res* 21: 199–209, 1993.
- Morikawa K, Ichihashi M, Kakiuchi M, Yamauchi T, Kato H, Ito Y, Gomi Y. Effects of various drugs on bladder function in conscious rats. *Jpn J Pharmacol* 50: 369–376, 1989.
- Morikawa K, Kakiuchi M, Fukuoka M, Kato H, Ito Y, Gomi Y. Effects of various drugs on bladder function in conscious restrained-denervated rats placed in a restraining cage and produced by transection of the hypogastric nerve. *Jpn J Pharmacol* 52: 405–411, 1990.
- Pacak K, Palkovits M. Stressor specificity of central neuroendocrine responses: implications for stress-related disorders. *Endocr Rev* 22: 502–548, 2001.
- Pikov V, Wrathall JR. Coordination of the bladder detrusor and the external urethral sphincter in a rat model of spinal cord injury: effect of injury severity. *J Neurosci* 21: 559–569, 2001.
- Robbins M, DeBerry J, Ness T. Chronic psychological stress enhances nociceptive processing in the urinary bladder in high-anxiety rats. *Physiol Behav* 91: 544–550, 2007.
- Simpson LA, Eng JJ, Hsieh JT, Wolfe DL, Spinal Cord Injury Rehabilitation Evidence Research Team. The health and life priorities of individuals with spinal cord injury: a systematic review. *J Neurotrauma* 29: 1548–1555, 2012.
- Smith AL, Leung J, Kun S, Zhang R, Karagiannides I, Raz S, Lee U, Glovatscka V, Pothoulakis C, Bradesi S, Mayer EA, Rodriguez LV. The effects of acute and chronic psychological stress on bladder function in a rodent model. *Urology* 78: e961–e967, 2011.
- Smith PP, Hurtado E, Smith CP, Boone TB, Somogyi GT. Comparison of cystometric methods in female rats. *Neurourol Urodyn* 27: 324–329, 2008.
- Spanos C, Pang X, Ligris K, Letourneau R, Alferes L, Alexacos N, Sant GR, Theoharides TC. Stress-induced bladder mast cell activation: implications for interstitial cystitis. *J Urol* 157: 669–672, 1997.
- Streng T, Santti R, Andersson KE, Talo A. The role of the rhabdosphincter in female rat voiding. *BJU Int* 94: 138–142, 2004.
- Thor KB, de Groat WC. Neural control of the female urethral and anal rhabdosphincters and pelvic floor muscles. *Am J Physiol Regul Integr Comp Physiol* 299: R416–R438, 2010.
- Weld KJ, Graney MJ, Dmochowski RR. Clinical significance of detrusor sphincter dyssynergia type in patients with post-traumatic spinal cord injury. *Urology* 56: 565–568, 2000.
- Yaksh TL, Durant PA, Brent CR. Micturition in rats: a chronic model for study of bladder function and effect of anesthetics. *Am J Physiol Regul Integr Comp Physiol* 251: R1177–R1185, 1986.
- Yoshiyama M, de Groat WC. Role of spinal metabotropic glutamate receptors in regulation of lower urinary tract function in the decerebrate unanesthetized rat. *Neurosci Lett* 420: 18–22, 2007.
- Yoshiyama M, deGroat WC, Fraser MO. Influences of external urethral sphincter relaxation induced by alpha-bungarotoxin, a neuromuscular junction blocking agent, on voiding dysfunction in the rat with spinal cord injury. *Urology* 55: 956–960, 2000.
- Yoshiyama M, Roppolo JR, Takeda M, de Groat WC. Effects of urethane on reflex activity of lower urinary tract in decerebrate unanesthetized rats. *Am J Physiol Renal Physiol* 304: F390–F396, 2013.